Molecular mechanisms of cellular mechanics†

Mu Gao,[ab] **Marcos Sotomayor,**[ab] **Elizabeth Villa,**[ac] **Eric H. Lee**[acd] **and Klaus Schulten***[abc]

Mechanical forces play an essential role in cellular processes as input, output, and signals. Various protein complexes in the cell are designed to handle, transform and use such forces. For instance, proteins of muscle and the extracellular matrix can withstand considerable stretching forces, hearing-related and mechanosensory proteins can transform weak mechanical stimuli into electrical signals, and regulatory proteins are suited to forcing DNA into loops to control gene expression. Here we review the structure–function relationship of four protein complexes with well defined and representative mechanical functions. The first example is titin, a protein that confers passive elasticity on muscle. The second system is the elastic extracellular matrix protein, fibronectin, and its cellular receptor integrin. The third protein system is the transduction apparatus in hearing and other mechanical senses, likely containing cadherin and ankyrin repeats. The last system is the *lac* repressor protein, which regulates gene expression by looping DNA. This review focuses on atomic level descriptions of the physical mechanisms underlying the various mechanical functions of the stated proteins.

Introduction

Biological cells utilize molecular compounds as well as mechanical forces as input, output, and signals. While the transformation of chemical compounds by cells, *e.g.*, through enzymes, has been studied for decades, much less is known about the transformation of mechanical forces. Just as cells transform chemical compounds, they also transform mechanical forces. Examples are motor proteins with forces as output,[1] F1 ATP synthase with torque as input,[2,3] or mechanosensitive channels with force as a signal.[4] The mechanical forces that arise in cells amount to a few pN in single proteins, but can be much larger in multi-protein filaments that experience cellular scale strain.

Obviously, the cell needs proteins that can sustain mechanical forces. Examples are the forces arising in sarcomeric muscle cells where the cell uses the protein titin[5,6] to maintain structural integrity and provide passive elasticity for the muscle sarcomere.

In order to detect mechanical forces as signals, cells need to respond to such forces through significant, yet reversible structural changes. Examples are the proteins, not yet unambiguously identified, that form the transduction apparatus in inner ear hair cells capable of detecting the weak acoustical forces arising in the cochlea.[7,8] Other examples are the transmembrane proteins involved in transduction of force signals across cellular membranes[9] and the extracellular matrix proteins designed to connect cells in tissues.[10]

Forces also arise within cells in numerous other circumstances where one might not expect them off-hand. An example is the regulation of the genome where, due to the macroscopic length of the cellular DNA, strong coiling forces arise that regulatory proteins need to sustain.[11] In fact, many regulatory proteins deform the DNA through formation of kinks and loops.[12]

What is the physical mechanism underlying the mechanical functions of proteins? To address this question one may follow the conventional route of inspecting equilibrium protein structures. However, in the present case such structures are of only limited value since they typically do not reflect the mechanical properties connected with significant structural deformation induced by forces. Fortunately, there exist today numerous experimental methodologies for directly probing mechanical responses of a single biopolymer. Key methods are atomic force microscopy (AFM),[13,14] laser optical tweezers,[15,16] fluorescence resonance energy transfer,[17–19] and biomembrane force probe.[20] It was due to these novel methods that the study of active and passive mechanical systems in cells experienced a rapid development; yet, all these methods reveal only very limited microscopic detail on biopolymer mechanics, *e.g.*, in the case of AFM experiments observables are only a rupture force value and the associated extension.[21] This is where molecular dynamics modeling can contribute significantly.

Molecular dynamics has the ability to probe the passive mechanical properties of proteins by application of external forces. The methodology, best known as steered molecular dynamics (SMD), has been developed over the last decade and achieved notable successes in relating structure, function, and

[a] *Beckman Institute, University of Illinois at Urbana-Champaign, Urbana, IL, USA. E-mail: kschulte@ks.uiuc.edu*
[b] *Department of Physics, University of Illinois at Urbana-Champaign, Urbana, IL, USA*
[c] *Center for Biophysics and Computational Biology, University of Illinois at Urbana-Champaign, Urbana, IL, USA*
[d] *College of Medicine, University of Illinois at Urbana–Champaign, Urbana, IL, USA*

observation to physical mechanisms permitting biopolymers, in particular proteins, to bear the forces arising from natural cellular processes.[22–45]

It is certainly not possible to cover all aspects of cellular mechanical processes in this short review. Instead, we choose four protein systems where SMD studies have provided crucial structural insights into the molecular mechanisms underlying the functions of these proteins. We discuss the mechanical properties of the protein titin that determines the passive elasticity of muscle, the elastic extracellular matrix protein fibronectin and its cellular receptor integrins, the proteins ankyrin and cadherin likely involved in mechanotransduction in the inner ear and other mechanical senses, and the *lac* repressor protein that regulates gene expression by looping DNA. We apologize to all researchers whose pioneering work cannot be reviewed due to the space limit.

Steered molecular dynamics

SMD is an ideal computational tool to probe mechanical properties of biopolymers at the atomic level. SMD can induce conformational changes on time scales covered by molecular dynamics simulations, *i.e.*, typically a few tens of nanoseconds. For this purpose, external forces are applied, *e.g.*, between the termini of a protein; the forces and the response of the biopolymer, *e.g.*, linear extension, are recorded and subsequently analyzed. The SMD approach, reviewed in ref. 26, 46, 47, has provided important insights into molecular mechanisms of cellular mechanics for ligand–receptor binding,[22–25,48] cellular adhesion,[27–29] force generation,[49] transduction of mechanical signals,[50–52] regulation of gene expression,[44,53] and protein elasticity.[30–39,41–43,54–56]

There are many ways forces can be applied in SMD simulations. This is achieved through protocols defining typically how force strength and direction varies as a function of time. In the simplest case one specifies a constant force; another typical protocol corresponds to connecting a set of atoms to a harmonic spring, the end of which is pulled with constant velocity.[26] Forces can also be applied interactively in an ongoing simulation by means of a so-called haptic device.[57,58] These and other force protocols have been implemented in NAMD,[59] the MD program employed in all the SMD studies reviewed here. The constant velocity SMD protocol mimics AFM experiments in which a molecule is stretched by a cantilever moving at constant velocity. This protocol easily induces conformational transitions since force can rise to very large values; this advantage is outweighed by the lack of explicit control of the force. The constant force SMD protocol permits selection of the force magnitude such that key conformational transitions, unresolved in constant velocity protocols, are captured in "slow motion". Through NAMD one can define linear forces as well as torque. In addition to these built-in features, NAMD also provides a scripting interface that allows one to customize SMD procedures for complex force protocols,[59] such as simulating the membrane surface tension acting on a mechanosensitive channel[51] or forces due to DNA looping acting on a regulatory protein.[44] The most flexible force protocol is available within interactive molecular dynamics simulations, in which case

linear force or torque can be issued and varied by the user on the fly in an ongoing simulation with visual and mechanical feedback.[57,58]

A limitation of the modeling approach, however, is the short time scale accessible to MD, several orders of magnitude shorter than the time scale of AFM observations. As a result, peak forces calculated in SMD simulations are typically one order of magnitude higher than those obtained from AFM experiments. Despite this difference, SMD simulations have generated trajectories with features that are in close agreement with AFM experiments, such as the extension of intermediates[33,41] and the relative mechanical stability of a group of proteins.[42] For a protein with multiple unfolding pathways under the same pulling geometry, SMD simulations can reveal these pathways and suggest mutants discerning pathways experimentally.[40,54,60] Extended simulation times lead to improved convergence with observation.[32] Nevertheless, one should abstain from focusing on peak forces when comparing simulation and observation and instead focus on energetics and related mean first passage times.[32,61]

The observables monitored in SMD simulations, typically force and extension as a function of time, need to be analyzed in terms of quantitative measures of protein mechanical properties such as elastic moduli or potentials of mean force (PMF) along a stretching direction. For this purpose analysis methodologies have been developed based on non-equilibrium statistical mechanics for the calculation of the PMF[61] and on mean first passage times.[22,32,40]

An extension-time profile obtained from a constant force SMD simulation usually displays plateaus corresponding to unfolding/unbinding barrier crossing processes. The length of a plateau indicates the first passage time spent in crossing the barrier. The applied force effectively lowers the barrier such that stronger forces lead to faster barrier crossing than weaker forces. In all cases, the stretching motion gets temporarily "stuck" in front of the barrier, which is then overcome by thermal fluctuations. This scenario can be described as Brownian motion governed by a potential which is the sum of the indigenous barrier and a linear potential accounting for the applied force. The mean time $\tau_{barrier}$ to cross the barrier can be evaluated using the expressions for the mean first passage time.[62–64] An analytical expression of $\tau_{barrier}$ exists for a linearly increasing ramp model for the PMF.[22] By comparing the mean first passage times with the respective times $\tau_{barrier}$ for various forces, one can estimate the height of the indigenous potential barrier. Using this approach, the height of the major unfolding barrier of titin I27[32] and fibronectin modules[37,42] have been estimated, the results being in close agreement with AFM experiments.[21,65]

The mean first passage time method for sampling trajectories from constant force pulling requires an estimate for the PMF and provides limited information regarding the PMF, mainly the height of the potential barrier associated with unfolding/unbinding. Based on the Jarzynski equality,[66–68] a new method for sampling trajectories obtained from constant velocity pulling has been proposed to reconstruct the PMF without any assumption on its shape.[69]

The Jarzynski equality relates the free energy difference $\Delta G = G_B - G_A$, where G_A and G_B correspond to the free energy

This journal is © the Owner Societies 2006

Phys. Chem. Chem. Phys., 2006, **8**, 3692–3706 | 3693

at states A and B, to work W enforcing the transition A $\rightarrow$ B through non-equilibrium processes. The equation reads

$$\exp(-\beta \Delta G) = \langle \exp(-\beta W) \rangle \qquad (1)$$

where $\beta = 1/k_B T$ is the inverse temperature and k_B is the Boltzmann constant. The Jarzynski equality provides a means to extract ΔG from averaging, denoted by $\langle \cdots \rangle$, over A $\rightarrow$ B non-equilibrium processes, such as SMD stretching. Unfortunately, the exponential average in eqn (1) is strongly dominated by instances in which small work values arise. Since such instances (trajectories) occur rarely, direct application of this equation to calculate a PMF is not practical. However, in case the work values follow a Gaussian distribution, the cumulant expansions of eqn (1) contributes only first and second order terms, which permits easy calculation of the exponential average.[69] In a SMD simulation performed with a stiff spring, the work on the system is indeed Gaussian-distributed and the 2nd order cumulant expansion of Jarzynski's equality can be applied.[69] This method for determining the PMF compares favorably with the widely used umbrella sampling method because of its easy implementation and uniform sampling.[70] The Jarzynski equality has been employed successfully to reconstruct the PMF characterizing the conduction of small molecules through channel proteins.[71,72]

Titin

An essential characteristic of striated muscle is its elasticity. Tiny muscle fibrils, known as myofibrils (1–2 μm in diameter), can be stretched to twice their resting length without damaging their structure. At the molecular level, the elasticity is due to a filament composed of a single gigantic protein, titin.[5,6] As shown schematically in Fig. 1, titin spans over half of the vertebrate striated-muscle sarcomere, the smallest self-contained functional unit of myofibrils. A typical titin molecule has a length of $\sim$1 μm and a molecular weight of up to $\sim$4 MDa. In fact, titin is the largest covalently linked protein encoded in the human genome. Sequence analysis suggests that titin is linearly assembled from about 300 modules of two types, immunoglobulin-like (Ig) and fibronectin type III

(FN-III), as well as a few other domains.[73,74] A unique PEVK domain (rich in proline (P), glutamate (E), valine (V), and lysine (K)) has a flexible secondary structure,[73,75] and becomes unfolded first upon stretching.[76,77] To prevent the high force developed in sarcomere, a few individual Ig domains in the I-band region of titin also become unfolded.[78,79]

The mechanical properties of titin Ig domains have been studied by means of AFM[14,21,33,79,81–83] and optical tweezers[84,85] as well as SMD simulations.[30,32,33,35,36,38,56,86] The combination of observation and simulation revealed that titin acts as a heterogeneous spring protected against rupture by the ability of individual domains to partially and completely unfold. In particular, computational modeling has provided important insights into the design principles of proteins that act as elastic elements and, at the same time, withstand the considerable forces arising from cellular mechanics. A classic example is the titin I-band Ig domain, I27 (or I91 in the new nomenclature[74]). SMD simulations[30,32,33,35] and AFM experiments[21,33,81,83] explained how the double β-sheet architecture of I27 is optimal for the desired mechanical properties—elasticity at short extension and protection against rupture through two-step unraveling (involving a mechanically stable intermediate state at about 10 Å extension and involving the completely unfolded state extending to about 300 Å). The force-bearing elements of I27 are inter-strand hydrogen bonds near the N- and C-termini; these bonds have to break concurrently before the stretched domain can extend further, the concerted bond breaking posing high energy barriers against extension. Altering the number of hydrogen bonds connecting force bearing, *i.e.*, terminal, β-strands permitted evolution to design domains of specific strength.

The computational work took advantage of two developments, the availability of an NMR structure of I27[87] and the rise of AFM, a methodology ideally suited for the investigation of titin domains.[14,21,33,79,81–83] SMD permitted direct comparison between simulations and AFM observations. These simulations led to experiments of I27 mutants which modulated the force bearing elements corroborating earlier findings.[33,88] In addition to these SMD studies employing explicit solvents, computational studies with simplified models
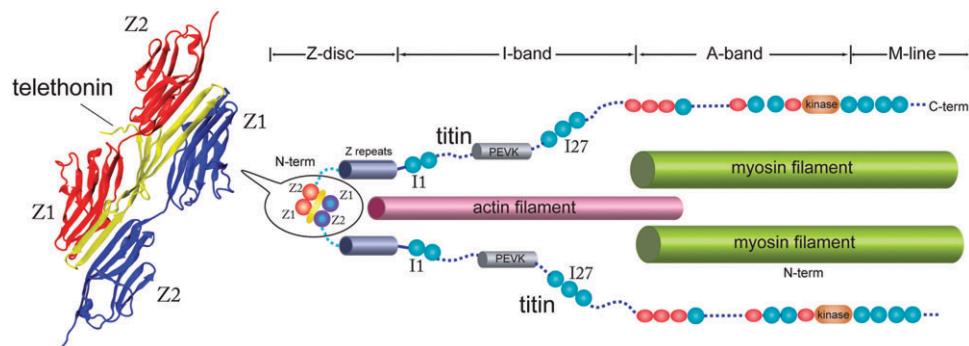

Fig. 1 Schematic overview of the muscle protein titin in the muscle sarcomere. The sarcomere contains three major filaments: actin filaments, myosin filaments, and titin filaments. The titin filaments connect to the actin filaments at the Z-disc and associate with the myosin filament over the A-band and M-line regions. The contractile movement of the sarcomere is due to the sliding of the myosin filament over the actin filament, while the unfolding of titin domains provide the extension for the sarcomere during stretching of the sarcomere. Note that only half of the sarcomere is shown. Ig and FN-III domains, two common structural motifs of titin, are represented by circles and ovals, respectively. The N-terminal Z1Z2 Ig domains of two titins (shown in blue and red circles) are connected through a protein called telethonin (yellow). The crystal structure of the complex is shown in cartoon representation (Protein Data Bank code 1YA5[80]).

have been reported, including an implicit solvent model[89,81] and coarse-grained models.[90,91]

A second titin I-band Ig domain that became structurally known is I1.[92] I1 exhibits, in particular, a strong network of ten inter-strand hydrogen bonds protecting against the extension of the domain's termini. The strength of the protection and the lack of an I27-like intermediate state was seen both in AFM measurements[82] and simulation.[38] I1 also contains two cysteine residues that can form a disulfide bridge in an oxidized environment, further protecting against extension of the protein. The simulations, comparing oxidized and reduced I1, demonstrated that this disulfide bridge increases the mechanical stability and limits the extension of oxidized I1.[38] This was then confirmed by AFM observation.[82]

One of the main surprises observed in the MD investigations of I1 and I27 was the essential role of water in rupturing titin domains: water molecules constantly attack and break inter-strand hydrogen bonds. Unraveling of I1 and I27 is only possible when a sufficient number of hydrogen bonds are broken by surface water such that the remaining bonds can be ruptured by the applied forces, *i.e.*, forces need water molecules as accomplices to unravel Ig domains.[35,38] This role of water seems to be typical in the unfolding of mechanical proteins.

The terminal regions of a titin spring are anchored at the Z-disc and M-line of a muscle sarcomere and interact with numerous proteins.[5,6] These titin-based complexes provide not only structural support for the development and function of myofibrils, but also play regulatory roles by detecting stretching force in titin.[93] A unique titin kinase at the C-terminal region, for example, exhibits a conformational change in response to mechanical force.[55,94] At the very end of the N-terminal region of titin, a sensor complex is formed based on two titin Ig domains, Z1 and Z2,[95] anchored through the ligand telethonin.[96–98] Biochemical characterization of telethonin has shown that its presence, in conjunction with titin Z1Z2, is required for progression of muscle growth.[97] Point mutations to telethonin resulting in premature stop codons have been correlated to a form of limb girdle muscular dystrophy (type 2A),[99–103] suggesting that telethonin plays a major role in the stabilization of N-terminal titin at the Z-disc.

While binding studies have shown that titin Z1Z2 associates with telethonin at the Z-disc, the specific arrangement of the interaction was not known until very recently when the structure of the N-terminal half of telethonin in complex with titin Z1 and Z2 became available,[80] as shown in Fig. 1. Unlike typical ligand binding through insertion of the ligand into a receptor pocket, the crystal structure revealed that the liganded Z1Z2 domains of two separate antiparallel titin N-termini are joined together by an N-terminal fragment of the ligand telethonin through β-strand cross-linking (see Fig. 1 and 2), a structural motif that also appears in pathological fibril formation.[104–107] On the other hand, it is known that β-strands can form mechanically stable β-sheets found in titin Ig domains or fibronectin type III like modules (reported above, and below). Naturally this raises the question: Does the β-strand cross-linking between titin and telethonin represent a novel ligand binding strategy that provides a mechanically stable linkage?

This question has been addressed by all-atom SMD simulations performed in order to understand the mechanical design of the Z1Z2–telethonin complex.[56] The simulations revealed that the Z1 and Z2 domains are bound strongly to telethonin. It turns out, in fact, that the Z1Z2–telethonin complex exhibits significantly higher resistance to mechanical stretching forces than titin Z1Z2 alone (see Fig. 2), suggesting that telethonin plays a role in anchoring titin to the sarcomeric Z-disc. Whereas previous studies have revealed that the unraveling of the β-strands for titin Ig-domains constitutes the dominant unfolding barrier,[86] in the case of Z1Z2 in complex with telethonin, the force peak observed corresponded to a detachment of one virtually intact Z2 domain from telethonin.

The results from these simulations shed light on a key structural strategy that the titin Z1Z2–telethonin complex employs to yield extraordinary resistance to mechanical stress. The major force bearing component of this complex is an extensive intermolecular hydrogen bonding network formed across β-strands between telethonin and Z1Z2 domains, and not intramolecularly between β-strands of individual Z1 or Z2 domains (see Fig. 2). This shift to a stronger force bearing interface reduces the chance of unraveling the individual Ig-domains, thus stabilizing the complex. This example demonstrates how β-strand cross-linking, *i.e.*, formation of an intermolecular β-sheet, serves as an important mechanism, in effect a molecular glue, for augmenting the ability of protein complexes to resist mechanical stress.

Fibronectin and integrin

Cells are connected through a network known as the extracellular matrix (ECM).[10] Many cellular processes involve interactions between the ECM and the cell. The ECM not only connects cells together in tissues, but also guides their movement during wound healing and embryonic development. Furthermore, the ECM relays environmental signals to cells. One essential component of the ECM is the protein fibronectin that assembles into fibrils attaching cells to the ECM.[108] Besides the fibrillar form, fibronectin also has a compact non-functional soluble form circulating in blood. The transformation from the compact form to the extended fibrillar form of fibronectin, a highly regulated process termed fibrillogenesis, requires application of mechanical forces generated by cells.[109] As shown schematically in Fig. 3, cells bind and exert forces on fibronectin through transmembrane receptor proteins of the integrin family,[9,110] which mechanically couple the actin cytoskeleton to the ECM *via* an elaborate adhesion complex.

Fibronectin fibrils exhibit salient elastic properties. Cells can stretch FN fibrils up to four times longer than their relaxed length.[18] The mechanical responses of FN are conferred by its multimodular structure composed predominantly of three different repeats termed FN-I, FN-II, and FN-III. Each of the two fibronectin subunits consists of 12 FN-I, 2 FN-II, and 15 to 17 FN-III modules, respectively. While each type I or type II module contains a couple of disulfide bonds that cross-link β-strands of the module, type III modules do not contain any disulfide bond. Structurally, FN-III modules exhibit a seven-β-stranded sandwich motif that has been found
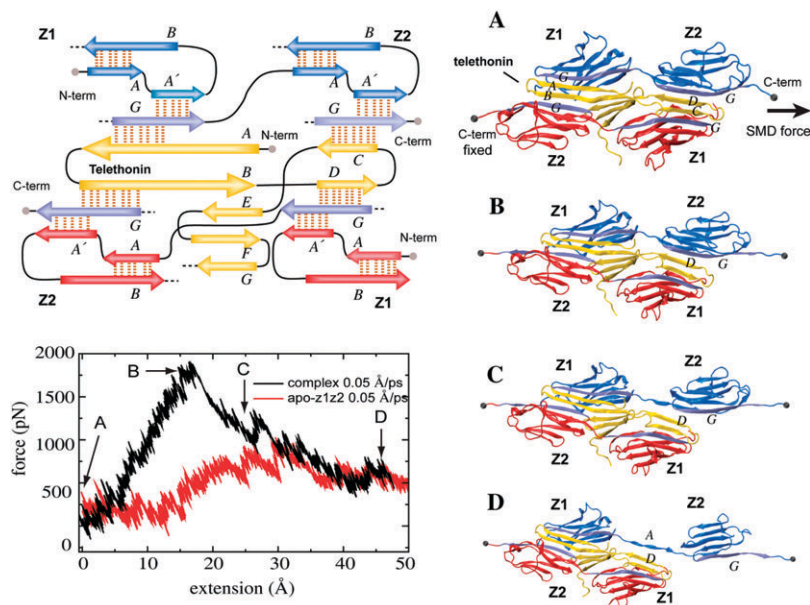
This journal is © the Owner Societies 2006

Phys. Chem. Chem. Phys., 2006, **8**, 3692–3706 | 3695

Fig. 2 Structure and mechanical stability of a telethonin-liganded titin Z1Z2 complex. Shown in the upper left is a schematic view of the β-strand alignment for the complex, with key force bearing hydrogen bonds shown for β-strand pairs AB and A′G of the titin Z1 and Z2 domains, and hydrogen bonds linking the four G-strands on the Z1 and Z2 domains to β-strands on telethonin. Shown in the lower left is the force–extension profile of the telethonin-liganded Z1Z2 complex and of an isolated Z1Z2 unit. The profile depicts the force needed in the constant velocity SMD simulations to stretch the systems to a certain extension relative to the equilibrium length. Shown on the right are snapshots of the titin–telethonin complex for various extensions. Comparing the force–extension profile one can see that unbinding the complex requires significantly higher force than unfolding an isolated Z1Z2 unit. The complex shown in snapshot (A) defines the initial state before stretching at 0.05 Å ps^{-1}. (B) At extension of 15 Å, a peak force is necessary for detaching the G-strand of a Z2 from its cross-linking partner, the D-strand of telethonin. (C) The Z2 domain becomes separated from the ligand at extension 25 Å. (D) Unraveling the Z2 domain leads to further separation. Hydrogen bonds are represented by dashed lines. Figure adapted from ref. 56.

ubiquitously in many mammalian proteins.[41,111,112] It has been proposed that individual FN-III modules unfold to provide the elasticity of FN fibrils.[113] Consistent with this hypothesis, experiments with dual-labeled fibronectin undergoing fluorescent resonance energy transfer show a marked reduction in energy transfer for fibronectin incorporated into extracellular matrix fibrils, supporting the notion that partial unfolding of FN-III modules occurs during fibrillogenesis.[114]

In addition to providing the necessary elasticity for accommodating cell movement, stretching of FN-III modules can expose buried binding sites that serve as nucleation sites for the assembly of FN into fibrils. These buried binding sites, called cryptic sites, presumably exist either within the FN-III core or buried between the hinge regions of two neighboring FN-III modules. Cryptic sites for fibrillogenesis have been proposed to exist in FN-III$_1$,[115,116] FN-III$_2$,[117] FN-III$_7$,[118]
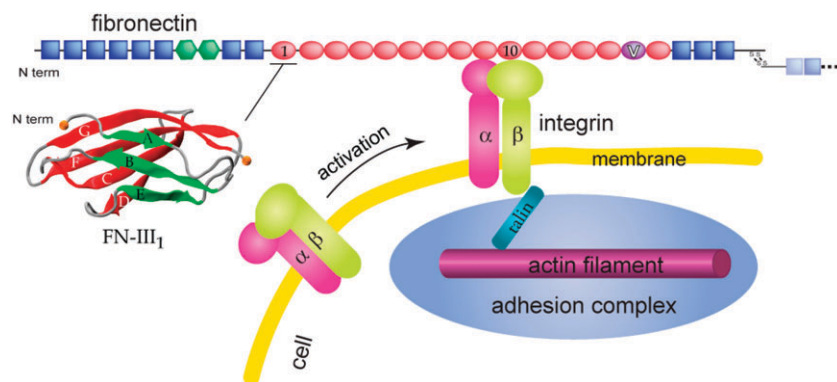

Fig. 3 Schematic view of fibronectin bound to integrin at the cell surface. Fibronectin is a dimeric protein consisting of two identical subunits cross-linked by disulfide bridges. One of the subunits, shown in the figure, is composed of type I (squares), type II (hexagons), and type III (ovals) modules, as well as of a variable (V) region. An atomic NMR structure of FN-III$_1$ (Protein Data Bank code 1OWW)[41] is shown in cartoon representation. Integrin is a heterogenous dimeric protein composed of two non-covalently associated subunits. Upon activation, integrin undergoes conformational changes and mechanically links its extracellular ligands, such as fibronectin, to an intracellular cytoskeleton adhesion complex, which involves dozens of proteins (*e.g.*, talin and actin).

FN-III$_9$,[119] FN-III$_{10}$,[120] and FN-III$_{13–15}$.[118,121] Thermal or chemical unfolding of these modules is associated with increased binding by either FN or a 70 kDa N-terminal FN fragment. Furthermore, a 76-residue fragment from FN-III$_1$, termed anastellin and obtained by cutting the protein A- and B-strands off the N-terminus, binds to fibronectin and promotes the formation of so-called superfibronectin with enhanced adhesive properties.[122]

Despite remarkably similar tertiary structures, distinct FN-III modules share low sequence homology, with the sequence identity being typically less than 20%. Conversely, the sequence homology for the same FN-III module across multiple species is notably higher, approximately 80–90%, suggesting that sequence variability among modules is functionally significant. The mechanical properties of individual FN-III modules have been compared in single molecule AFM experiments[65,123–126] and in all-atom SMD simulation studies.[34,37,39–42] The AFM experiments revealed varied mechanical stability of FN-III modules. The relative order of the observed stability is qualitatively consistent with the prediction obtained from SMD simulations of several FN-III modules FN-III$_{7–10,12–14}$, and a FN-III module from tenascin.[42] The simulation results have shown that FN-III modules can be pre-stretched with only minor changes to their tertiary structures before encountering the major unfolding barrier, and the mechanical stability of FN-III modules can be tuned through substitutions of just a few key amino acids by altering access of water molecules to inter-strand hydrogen bonds that break early in the unfolding pathway.

More interestingly, the AFM experiments with FN-III modules revealed that the mechanical response of FN-III$_1$ is markedly different from that of other FN-III modules such as FN-III$_{10}$, FN-III$_{12}$, and FN-III$_{13}$.[65] FN-III$_1$ exhibits a pronounced mechanical intermediate during forced unfolding. While a similar intermediate has been detected for other FN-III modules such as FN-III$_{10}$, it was observed less frequently than that of FN-III$_1$.[60] A combination of NMR structural analysis and molecular modeling provided a structural explanation of this particular property of FN-III$_1$.[41] Homologous to other structurally solved FN-III modules, FN-III$_1$ consists of two four-stranded β-sheets packed into a β-sandwich motif. Unlike most other FN-III modules, however, FN-III$_1$ misses in its G-strand a well conserved proline residue among FN-III modules. As a result, the key force-bearing inter-strand hydrogen bonds of the CDFG β-sheet of FN-III$_1$ is extended. Thus, the β-sheet becomes much more stable than the ABE β-sheet (Fig. 4). Upon tension, the weaker ABE β-sheet unravels first. The N-terminal portion of the module, the A- and B-strands, completely extend to ∼100 Å, three times the native length of a typical FN-III module. This new conformation amounts to a stable intermediate with the stronger β-sheet protected by a cluster of inter-strand hydrogen bonds between G- and F-strands. The extension difference between native state and intermediate is in agreement with atomic force microscopy unfolding experiments;[65] the intermediate structure predicted by the simulations is surprisingly close to the structure of anastellin, the 76 N-terminal portion of FN-III$_1$.[127]

Fibronectin is recognized by integrins α5β1 and αVβ3.[128] The primary sequence motif of fibronectin for integrin binding
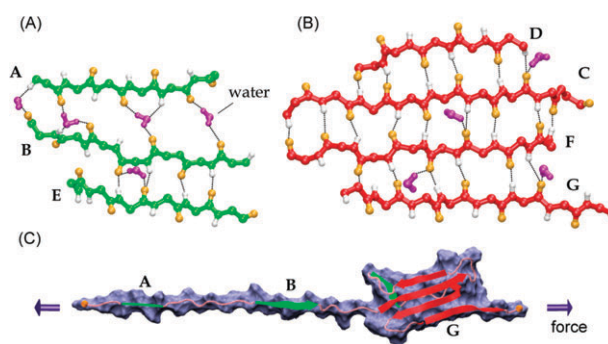

Fig. 4 Stretching the FN-III$_1$ module. The overall structure of FN-III$_1$ is shown in Fig. 3. SMD simulations, which started from an NMR structure of the protein (Protein Data Bank code 1OWW), revealed that the module consists of two β-sheets with different mechanical strength.[41] (A) The weaker ABE β-sheet (green) unravels first when force is applied to the termini of the module, while (B) the stronger CDFG β-sheet (red) still maintains its inter-strand hydrogen bonding network. Unraveling of the A- and B-strands leads to (C) a stable mechanical intermediate with the stronger β-sheet largely intact. Hydrophobic residues exposed in this intermediate likely bind to other fibronectin modules, thereby enabling the self-assembly of fibronectin molecules. Hydrogen and oxygen atoms are colored in white and yellow, respectively. Panels (A) and (B) were adapted from ref. 41.

is a tripeptide, Arg-Gly-Asp (RGD), located on the loop connecting the force-bearing G- and F-strands of FN-III$_{10}$. Multiple mechanical unfolding pathways have been observed in the SMD studies of this module because either of its two β-sheets may become unraveled first, or the sheets may become disrupted simultaneously.[34,40] In the most common pathway, the G-strand near the C-terminus detaches from the module, inducing a gradual shortening of the distance between the apex of the RGD-containing loop and the module surface, which reduces the loop's accessibility to surface-bound integrins. The shortening is followed by a straightening of the RGD loop from a tight β-turn into a linear conformation which implies a further decrease of the affinity and selectivity to integrins. In a second pathway, FN-III$_{10}$ exhibits an intermediate similar to that observed in the simulations of FN-III$_1$ (see above). The RGD loop maintains its initial conformation until disruption of this intermediate. These observations suggest that the RGD loop is strategically located to undergo conformational changes and constitute a mechanosensitive control of integrin recognition.[34]

Besides the RGD peptide on FN-III$_{10}$, FN-III$_9$ also contains a short peptide that binds to integrin α5β1. This site, a so-called synergy site located about 32 Å from the RGD peptide, acts together with the FN-III$_{10}$ binding site to enhance integrin-mediated cell adhesion.[129] An SMD study of the FN-III$_{9–10}$ tandem has shown that fibronectin–integrin binding interactions can be affected through the change of the relative distance between the two sites upon stretching.[39] Prior to force-induced unfolding of the modules, the simulations revealed an intermediate state in which the synergy–RGD distance is increased to approximately 55 Å while both the conformations of the RGD loop and the synergy site themselves remain unperturbed. This synergy–RGD distance is too large for the RGD loop and the synergy site to co-bind the
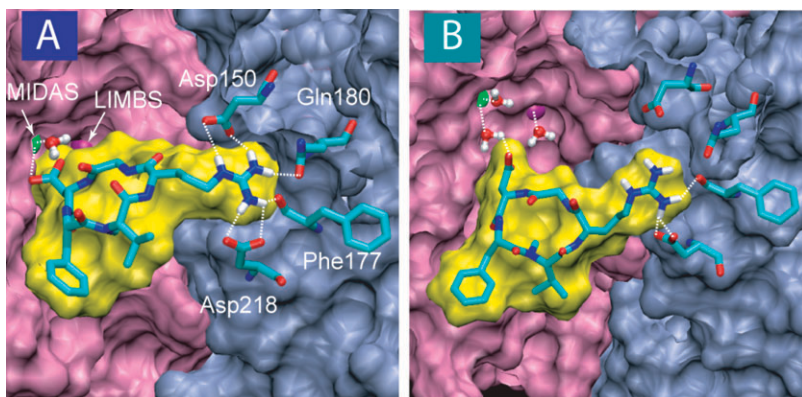
This journal is © the Owner Societies 2006

Phys. Chem. Chem. Phys., 2006, 8, 3692–3706 | 3697

Fig. 5 Forced dissociation of a cyclic RGD mimetic ligand from the binding site of its receptor integrin αVβ3. The two subunits of integrin αV and β3 are colored blue and purple, respectively. (A) Prior to the detachment of the ligand, the Asp of the RGD ligand contacts the MIDAS divalent cation, coordinated by β3 and a water molecule. The water molecule blocks access of other water molecules until (B) the separation of the Asp and the MIDAS ion, which triggers the dissociation of the ligand. Figure adapted from ref. 29.

same receptor molecule; they are thus functionally decoupled. The simulations suggest that increased α5β1 binding contributed by the synergy site, and associated downstream cell signaling events, can be turned off mechanically by stretching the two FN-III modules.

Naturally, the binding between integrin and fibronectin must sustain significant stress in order to transmit force signals. Indeed, AFM experiments have found that disruption of the α5β1–FN-III$_{7-10}$ complex requires strong force.[130] It has been known for a long time that integrins recruit divalent cations for the ligand binding purpose.[131,132] Crystal structures of integrin αVβ3, available recently both in the presence and absence of a synthetic RGD ligand, provide the first atomic view of how this integrin interacts with RGD-containing ligands.[133,134] The integrin acquires three divalent metal ions that coordinate the binding to the ligand. The Asp of the RGD peptide establishes a direct contact with the ion located at a site termed the metal ion dependent adhesion site (MIDAS, Fig. 5), which is flanked by two neighboring ions located at the ligand-associated metal binding site (LIMBS) and the adjacent MIDAS (ADMIDAS). While the exact role of the latter two sites is not clear, it has been shown that ADMIDAS regulates the binding affinity to the ligand.[135]

Based on the crystal structure of the complex, computational modeling of the RGD-ligand unbinding process has produced a dynamic picture of how the αVβ3 complex resists dissociation by mechanical forces.[29] Consistent with the hypothesis that integrin–ligand binding provides a stable mechanical linkage, the unbinding requires a high force comparable to the peak force observed in the unfolding of the strongest FN-III modules. This major force peak correlates with the breaking of the contact between the Asp of the RGD ligand and the MIDAS ion, as shown in Fig. 5. RGD binding to integrins does not involve a deep binding pocket that protects force-bearing contacts from attacks by free water, but rather forms a shallow crevice at the interface between the two subunits. A water molecule is tightly coordinated to the divalent MIDAS ion, thereby blocking access of free water molecules to the critical force-bearing interactions. A similar scenario has been found through molecular dy-

namics simulations in the complex of anthrax toxin with its cell surface receptor, the primary binding site of the latter also involving a MIDAS motif.[136]

Proteins related to hearing and other mechanical senses

The sense of hearing in vertebrates employs mechanically sensitive hair cells of the inner ear that transduce weak mechanical stimuli produced by sound into electrical signals.[137] These specialized cells located in the organ of Corti, on top of the basilar membrane of the cochlea, exhibit bundles of stereocilia arranged in rows of increasing height. The stereocilia become agitated in response to sound, resulting in concerted bending of the bundle accompanied by depolarization/hyperpolarization of the corresponding hair cell.[138,139] Fig. 6A and B show the current model explaining the mechanism of sound transduction.[7,137,140] Mechanosensitive ion channels in adjacent stereocilia are connected through a fine filament, termed the tip link,[141] as well as to the cytoskeleton. Bending towards the tallest stereocilia induces stretching of the tip link and opening of mechanosensitive channels, the latter event mediated by a "gating spring", as suggested by measurements of bundle elasticity.[142,143] While the microscopic cellular structures described are well understood, the molecular identity and corresponding elasticity of the different components of the transduction apparatus (tip link and mechanosensitive channels, either of which may form part of the gating spring) remains elusive and the subject of intense research.[144]

Motivated by experimental evidence suggesting that the tip link was made of cadherin-23[7,145,146] and the transduction channel was likely a member of the TRP ion channel family featuring numerous ankyrin repeats (TRPA1 and TRPN1 with up to 17 or 29 ankyrin repeats, respectively[8,151–153]), the elasticity of both cadherin and ankyrin repeats was extensively studied using SMD simulations.[43] The outcome of the simulations, recently corroborated by AFM experiments,[154,174] showed remarkable and novel properties for both ankyrin and cadherin, as described below. However, the role of these proteins in hair cell mechanotransduction remains ambiguous
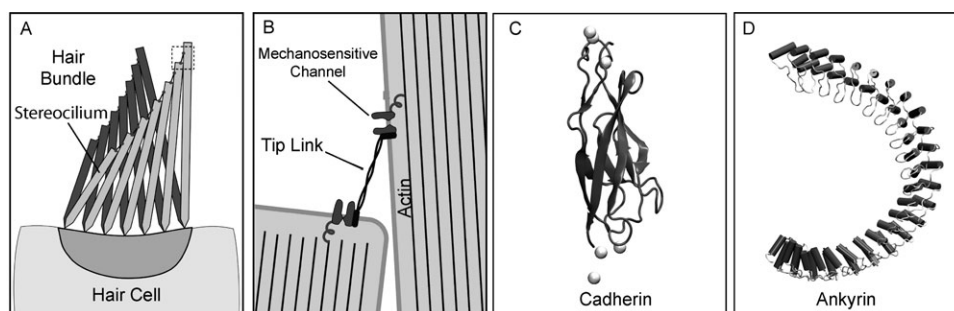
Fig. 6 Mechanotransduction in hair cells. (A) The side view shows the stereocilia arranged in order of increasing height. Deflection of a hair cell's bundle induced by sound causes the stereocilia to bend and the tip links between them to tighten. (B) Mechanical coupling of hair cell ion channels. Ion channels open in response to tension conveyed by tip links. The mechanism shown, involving a TRP type channel with an N-terminal ankyrin segment linked to the cell's cytoskeleton, is hypothetical. (C) Crystal structure of a single extracellular cadherin repeat. Calcium ions are shown as spheres. Transient lateral links (not shown) or the tip link are thought to be made of at least 54 extracellular heterogeneous cadherin repeats.[7,145–150] (D) Model of 24 ankyrin repeats of human ankyrin-R. Each repeat is made of two α-helices and a short loop.

as more recent experiments suggest that cadherin-23 is a component of transient lateral links of hair cells, but not the tip link.[147–150] Moreover, TRPN1 is unlikely to be the transduction channel in hair cells;[155] TRPA1 knockout mice exhibit normal balance and auditory response,[156–158] indicating that TRPA1 is not essential for hair cell mechanotransduction. Although poly-ankyrin domains of TRPA1 and TRPN1 homologues are unlikely to form the hair cell gating spring as originally suggested,[7,43,159] their elastic properties may be relevant in cold reception and mechanical nociception, as well as in mechanotransduction by sensory neurons.[160]

Despite the uncertainties about the specific role of cadherin repeats in hearing, the structural integrity of cadherin-23 is relevant for hair-cells, as demonstrated by mutations of *CDH23* causing hereditary deafness (Usher syndromes).[161,162] The mutations are indeed located in the extracellular domain of cadherin-23, formed by 27 heterogeneous repeats which may constitute the tip link or transient lateral links. The protein also features a domain crossing the cell membrane, and a domain located in the cytoplasm of the hair cell.[163] Each extracellular repeat consists of about 100 amino acids sharing a common folding topology characterized by seven antiparallel β-strands tightly linked by hydrogen bonds, and a highly conserved calcium binding motif (Fig. 6C).

The ankyrin segments of TRPA1 and TRPN1 are thought to consist of up to 29 similar repeats, each made of 33 amino acids.[8,151,152] Ankyrin repeats occur in more than 400 human proteins expressed in many tissues,[164–167] each repeat being made of two short antiparallel α-helices and a flexible loop (Fig. 6D). Proteins of the ankyrin family contain up to 24 repeats, and the largest ankyrin-repeat crystallographic structure available to date involves twelve of the repeats from human ankyrin-R; a structure with 24 repeats was extrapolated from it through modeling.[168] As Fig. 6D shows, adjacent ankyrin repeats stack in parallel and feature a slight helical curvature.[168–171]

The first characterization of the elastic response of cadherin and ankyrin repeats at the molecular level was performed using multiple SMD simulations.[43] Following earlier work on cadherin homophilic adhesion,[28] the new simulations revealed that a single cadherin domain (from C-cadherin[172]) is likely a stiff element that responds to an external force by independently unfolding its two β-sheets. The large forces required to unfold these domains were found to depend on the presence or absence of Ca^{2+} ions, pointing out the role of calcium as a structural stabilizer (Fig. 7A). A more recent study investigated the dynamics of two adjacent cadherin domains from E-cadherin and confirmed the relevance of calcium ions on the conformational flexibility of these proteins.[173] Interestingly, residues involved in calcium binding motifs are related to hereditary deafness,[161,162] *i.e.*, the respective mutations may undermine the ability of the tip link or transient lateral links to withstand large forces and/or form homophilic contacts.

In contrast, stacks of ankyrin repeats containing 12, 17, and 24 repeats were found to be flexible elements that respond to weak forces (25–100 pN) by changing their overall curvature and, despite two-fold elongations, keep their secondary structure intact; we refer to this property of ankyrin as "tertiary structure elasticity" (see Fig. 7B). The stiffness of ankyrin repeats observed in simulations (~ 5 mN m^{-1})[43] is in excellent agreement with the stiffness measured through AFM experiments (~ 4 mN m^{-1}).[174]

The simulations also showed that the response of ankyrin repeats to weak forces is reversible on a nanosecond time scale. External forces and constraints applied during stretching were turned off, permitting the protein to relax for several nanoseconds. During the relaxation, the end-to-end distance decreased considerably (by more than 40 Å during 25 ns for a system of 340 000 atoms containing the solvated 24 repeats of human ankyrin-R) and the original curvature was recovered.[43]

Application of large forces on ankyrin induced detachment and unfolding of individual repeats; we refer to this property, spectacularly represented by titin and fibronectin (see above), as "secondary structure elasticity". The simulations predicted that unfolding events can be identified as force peaks in constant-velocity stretching or as steps in constant-force stretching, since both force peaks and steps are separated by ~ 95 Å. Thus the end-to-end distance of unfolded poly-ankyrin domains could easily reach a maximum extension of ~ 2000 Å while still conserving entropic stiffness and reversibility.[43] These theoretical predictions have also been confirmed by AFM experiments on stacks of 6, 12 and 24 ankyrin repeats.[154,174]
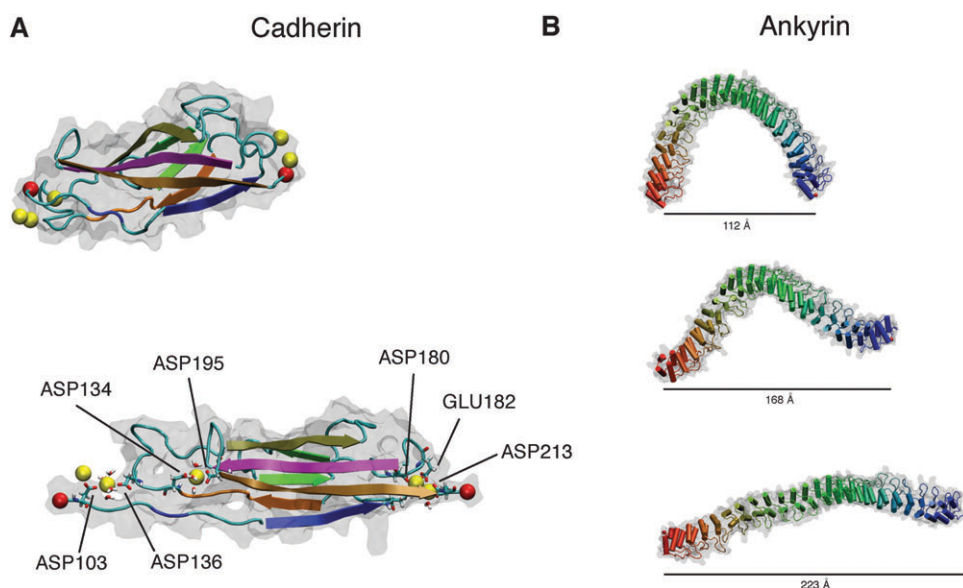
Fig. 7 SMD simulations of cadherin and ankyrin. (A) Equilibrated crystal structure of cadherin (from Protein Data Bank 1L3W)[172] (top) and partially stretched conformation (bottom) shown in cartoon representation. Specific residues and water molecules surrounding calcium ions (yellow spheres) are labeled and shown in licorice representation. (B) Equilibrated model of 24 ankyrin repeats of human ankyrin-R (top, 340 000 atom system, water not shown). Snapshots of the 24-repeat structure at the end of 10 ns constant-force simulations using forces of 25 and 50 pN (middle and bottom). The 24 ankyrin repeats were constructed from Protein Data Bank 1N11.[168]

Lac repressor

The mechanical manipulation of DNA is central to all aspects of genetic regulation.[11] Indeed, very often regulatory proteins mechanically manipulate DNA away from its equilibrium configuration by making DNA bend, loop, twist, and super-coil.[12] Examples of proteins or protein complexes that induce a change in DNA structure include the histones,[175] the protein component of the invertasome,[176] and the *lac* repressor (LacI).[177] In order to manipulate DNA, proteins need to overcome mechanical strain arising from the DNA. Little is known about how regulatory proteins are designed to handle the forces stemming from DNA. In many cases, conformational changes of DNA are known to occur in protein–DNA complexes, but cannot be resolved in detail when changes are too large or when the DNA becomes disordered. This is the case, in particular, when regulatory proteins force DNA into loops.

DNA looping arises when two distant segments of DNA are bound by a regulatory protein or protein complex. Such looping is widely observed in gene regulation, both in pro-karyotes[11,180] and eukaryotes.[181] DNA looping enhances both the regulatory properties of the proteins and the ability of the cell to respond to a wide range of signals.[12,182] Specifically, proteins and protein complexes involved in transcription in-hibition employ looping to influence the initiation process by blocking the promoter sequence, a site upstream from the genes that the RNA polymerase recognizes before initiating transcription.[183] The regulatory proteins act at different binding sites on the DNA, some of them distant from the promoter, exploiting the flexibility of DNA to bring themselves in close proximity in order to block the promoter. Proteins in this category include the *lac* repressor[177] shown in Fig. 8, and the *λ* repressor.[181]

The *lac* repressor mentioned above regulates the function of the *lac* operon in *Escherichia coli*, a set of genes involved in lactose catabolism.[182] Crystallographic structures of LacI bound to its DNA binding sites were reported, but neither of them contained the DNA loop.[178,179] Therefore, it is unclear
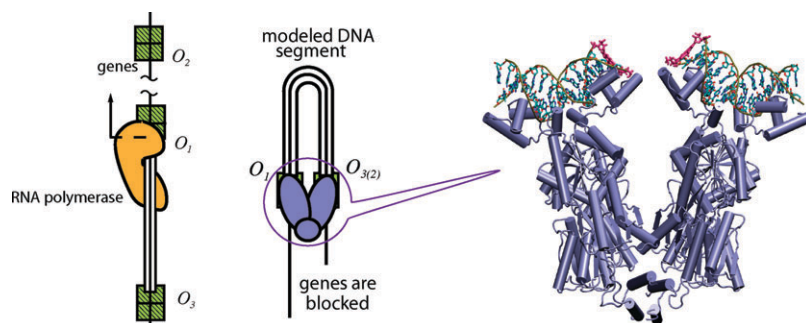

Fig. 8 Example of genetic regulation by the *lac* repressor. Shown is a schematic view of the *lac* operon when expressed (left) and repressed (middle). LacI binds to two operator sites on the DNA and forms a loop with the intervening DNA. The crystallographic structure of LacI[178,179] is shown on the right (Protein Data Bank code 1Z04).[188]

what the mechanics of repression are, given that the resistance of the connecting DNA loop is likely to change the structure of LacI. A suitable method for obtaining the missing details is molecular modeling starting from the known structural elements.

While SMD simulations could be applied directly to the study of muscle and hair cell protein systems involving 100 000 and 300 000 atom systems, the solvated *lac* repressor–DNA complex is currently beyond the reach of all-atom simulations. The protein by itself encompasses over 300 000 atoms when placed in a solvent bath sufficiently large to permit functionally important motions. For the DNA bound to the protein at its O1 and O3 operator sites and with a 76 bp loop between the sites (see Fig. 8) to have sufficient solvent space to freely move requires additional 500 000 atoms in a simulation. One also expects that the loop dynamics naturally impeded by the solvent is slow on the MD nanosecond time scale. In order to avoid extremely long 800 000 atom simulations, one resorts to a multiscale description in which the protein is described by all-atom MD and the DNA by a well-established physical model, the elastic rod model;[185] both descriptions are linked computationally, the DNA loop adapting instantly to the protein, but also exerting forces on the protein.

Such a multiscale methodology[53] has been developed based on earlier work on the DNA elastic rod model.[185–188] The approach is illustrated in Fig. 9. One can discern that the MD simulation involved the *lac* repressor bound to two short DNA segments. The segments continue into the DNA loop through the physical model that takes the segments as input (as boundary conditions for solving a system of 13th order non-linear differential equations) and yields as output the energetically optimal loop geometry along with the forces with which the DNA resists loop formation. Just like in an SMD simulation, the forces are included in the MD description of LacI. The elastic model accounts for the relevant properties of DNA, *i.e.*, intrinsic twist, bending anisotropy, and electrostatics.[185–188]

The multiscale method has been applied to the LacI–DNA complex.[53] For this purpose, an all-atom model of LacI has been built based on available crystallographic and NMR data, which were either low in resolution or missing parts of the protein.[178,179,189] The model of LacI, shown in Fig. 8, was reported in ref. 188.

LacI is assembled as a dimer of dimers, connected by a four-helix bundle. Each dimer has a head group that binds to DNA. Although binding of a single head group decreases expression, repression is most efficient when the loop is present.[190] The available[178] and modeled structure[188] (see Fig. 8) both include two 16 bp DNA segments nearly identical to the operators, but have the DNA loop missing. A mathematical DNA model predicted the structure of the missing loop.[186,188]

The DNA binding sites of LacI exhibit palindromic symmetry, giving rise to four possible binding orientations of DNA referred to as II, IO, OI, OO (see Fig. 9), two of which (II, OO) are equivalent when the sequence of the DNA in the loop is not considered. This gives rise to three different loop topologies represented also in Fig. 9. The generally accepted loop topology is IO[178,191] which is also the one simulated in ref. 44. However, there is no conclusive data excluding the
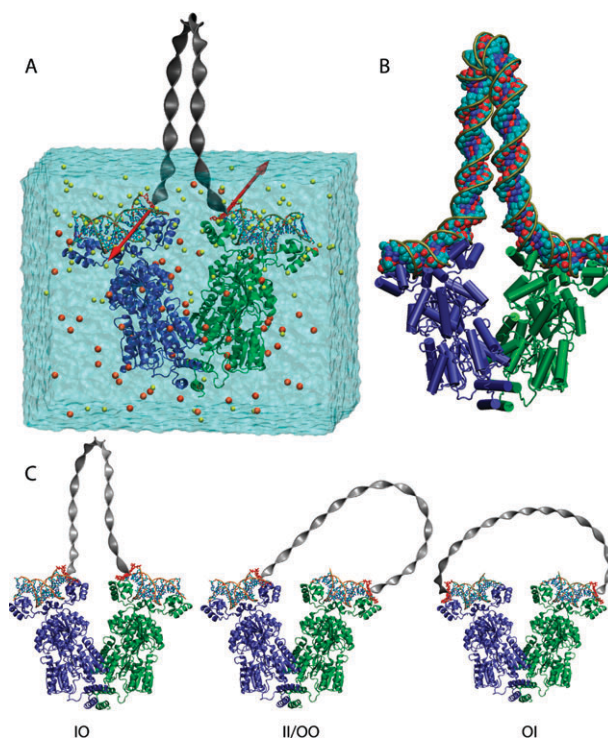

Fig. 9 Simulation of the *lac* repressor–DNA complex. (A) Setup of the multiscale simulation: all-atom structure of the complex between LacI and DNA in a bath of water and ions; the 75 bp-long DNA loop connecting the protein-bound DNA segments is modeled as an elastic ribbon; the forces of interaction between the loop and the protein-bound DNA segments (see arrows) are included in the MD simulation. (B) All-atom structure of the lacI–DNA complex. (C) Alternative topologies of the DNA loop formed by LacI based on orientation of the operators in the head groups. I denotes the 5′–3′ direction pointing toward inside the protein, and O denotes the 5′–3′ direction pointing away from the other head group. Notation adopted from ref. 184. The II and OO topologies are equivalent in our model that neglects a sequence dependence of DNA elastic properties.

other topologies. The structure of the DNA loop for all topologies was obtained from the boundary conditions of the all-atom system.[53] Based on the energetics of the DNA loops, the II/OO loop also appears a feasible candidate for the topology of the loop *in vivo*.

The results of the multiscale simulations of the IO loop–LacI construct corrected a long held view of the mechanism of LacI. While it was assumed previously that a hinge-like massive motion between the dimers controlled the ability of LacI to enforce the DNA loop, the simulations suggest that the ability of LacI to maintain the DNA in a looped configuration is actually due to the extreme flexibility of its head groups (DNA binding domains) connected to the rest of the protein through flexible linkers, while the dimers are essentially immobile with respect to each other. This is illustrated in Fig. 10 showing the head groups rotation and loop dynamics along with a moment of inertia of the LacI head group. The structure of the loop itself relaxed during the simulation, showing an energy drop from $\sim$20 $k_\mathrm{B}T$ to 12 $k_\mathrm{B}T$.[44] Interestingly, the computationally modeled behavior is in perfect agreement with experimental data, even though those same

This journal is © the Owner Societies 2006

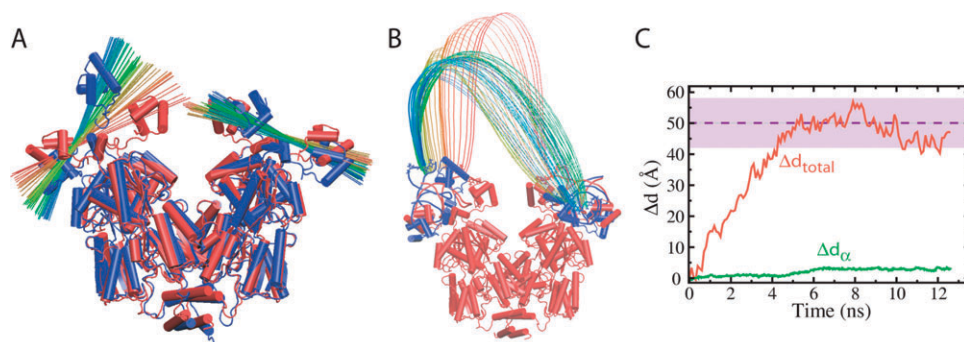*Phys. Chem. Chem. Phys.*, 2006, **8**, 3692–3706 | 3701

Fig. 10 LacI head group and DNA loop motion during the multiscale simulation. The protein structure is shown before and after the simulation. The lines in (A) represent the long principal axis of each head group after every 200 ps of the simulation. The structure of the DNA loop in (B) is drawn with the same frequency. (C) The distance d between two fluorophores attached to the DNA loop in ref. 191. Δd_{total} shows the change in d during the simulation; Δd_{α} shows how d would change if the head groups were immobile with respect to the core domains. The mauve band with the dotted line shows the experimental range and the average estimated for d.[191] Figure adapted from ref. 44.

data were interpreted differently before. Edelman and collaborators[191] have determined the distance between fluorophores attached to the DNA loop near the LacI head groups to be 50 Å larger than the same distance in the crystal structure;[178] this was ascribed to an opening of the LacI cleft when LacI actually binds to a DNA loop, which it does not in the crystal.[178,179] However, as shown in Fig. 10 the corresponding increase in distance by 52 Å measured in the simulation also explains the experimental observation without invoking a significant opening of the cleft.

Another multiscale simulation that forced LacI to open by applying external forces to the outer DNA ends, mimicking single molecule experiments,[192–194] revealed details of the mechanism of repression: when LacI is subject to strain from the DNA loop, a "lock" mechanism kicks in and prevents the cleft from opening. The locking mainly involves three groups of protein residues, that account for 80% of the dimer-to-dimer interaction energy. The interaction is mainly electrostatic, involving the formation of two salt bridges when the protein is subject to strain and locking it through a "catch-bond".[195]

As pointed out already, the DNA loop of the LacI–DNA complex can, in principle, also assume alternative topologies as shown in Fig. 9. The structure and energies of the OI and II/OO loops have been calculated.[53] The calculations show that the energy of the II/OO loop is comparable to that of the IO loop, while the OI loop appears energetically unfavorable in the LacI conformation tested. Investigation of the dynamics of the loops and the response of the protein to the respective forces will answer the question if the alternative loops are feasible. Given the wide rotational flexibility of LacI's head groups (see above), the differences in loop topology may be irrelevant since, through head group twists, one loop form, *e.g.*, IO, can be transformed approximately into another one, *e.g.*, II.

Outlook

The living state of a biological cell manifests itself through mechanical motion on many length scales. Behind this motion are many processes that generate and transform mechanical forces of many types. As with other cell functions, the machinery for cellular mechanics involves proteins. Their flexible structures, which can be deformed and restored, are often essential for their functions. In this review we considered a few mechanical proteins and demonstrated what had been learned about them through computational modeling. Regarding the examples given we now describe what the future may hold in store.

A few mechanical proteins take their flexibility to extremes by unfolding part of their structures. Examples reviewed here are the giant protein titin, the extracellular matrix protein fibronectin, and the repeat protein ankyrin. These molecular springs exhibit elasticity that come from their modular designs. The proteins respond to weak force by straightening the linker regions between modules. The ensuing elasticity is conferred by re-arrangement of the tertiary structure, and is called tertiary structure elasticity. Under strong force, individual modules unravel, unfolding secondary structure. The corresponding property is termed secondary structure elasticity. A typical structural motif for modules with secondary structure elasticity is the β-sandwich motif found in titin and fibronectin. The motif shows how mechanical proteins derive their mechanical strength, *i.e.*, resistance to unraveling under stretching through an interstrand hydrogen-bond network.

The β-sandwich is one of the most abundant protein structure motifs. The ground-breaking AFM experiments and SMD simulations of titin Ig domains and fibronectin type III modules have revealed a general mechanism for how a typical β-sandwich protein resists mechanical force: β-strands formed in the terminal regions of the protein are typically crucial force-bearing elements. The mechanical strength of individual β-sandwich modules can be tuned through variation of amino acids in these key β-strands. Moreover, some β-sandwich proteins, such as FN-III modules, exhibit stable mechanical intermediates that adhere to each other to form fibrils. Although it is not clear precisely how these modules cross-link, one possible way involves β-strand cross-linking.[119] As revealed in the structure and simulations of the titin Z1Z2–telethonin complex, β-strand cross-linking is a fundamental architectural element used by cells to glue their molecular components together yielding strong mechanical

connections. This structural motif has also been implicated in pathological fibril formation.[196] Clearly, the deployment of fibronectin, telethonin, and other similar mechanical proteins as powerful glue needs to be carefully controlled in the cell and future work will likely focus on the control mechanisms used in gluing the right protein components, and not the wrong ones, avoiding, in particular, self-aggregation.

Integrins, signaling receptor proteins, are vital players involved in transducing mechanical force signals across the cell membrane between the intracellular cytoskeleton complex and the extracellular matrix. Maintaining a stable mechanical linkage between integrins and their extracellular matrix ligands, as demonstrated in SMD simulations, is important for mechanotransduction. Furthermore, inactivated integrins, namely, the receptors in the absence of bound ligands, may be activated by mechanical force exerted on the cytoplasmic tails of integrins, opening sites that bind to the receptors.[9] Such force signals trigger conformational changes cascading to the integrin headpiece,[197–199] thus activating the receptors. The essential structural components of integrins for relaying and regulating conformational changes and cellular signaling are still not clearly understood.

Repeat proteins such as ankyrin are recognized today as ubiquitous components of biological cells. Examples are proteins made of leucine-rich repeats (LRR), armadillo repeats, and heat repeats like internalin, decorin, importin-β, exportin, clathrin, or catenin. These proteins resemble in a striking manner the overall curved architecture of ankyrin and likely exhibit secondary and tertiary structure elasticity similar to those of ankyrin. Do these repeat proteins have mechanical functions? If they do, how do their elastic properties serve their functions? One interesting case is the leucine rich repeat (LRR) domain of internalin from the bacterium *Listeria monocytogenes*.[200] The bacterium utilizes the rubber-band-like LRR domain to grip firmly a cellular receptor, E-cadherin, on the surface of a host cell. For such a system, SMD simulations provide a viable means to probe the elasticity of the structure and investigate how uncurling the LRR domain may affect the binding strength to its receptor. Another interesting example of repeat proteins with mechanical function are transport receptors associated with the nuclear pore complex.[201] The transport receptors embrace cargos, deliver them across the nuclear pore, and release them. The recognition of the transport receptor importin-β and transport factor NTF2 by nuclear pore complex proteins has been reported recently.[202,203] The mechanical flexibility of the transport receptors is thought to be important for its function and is under investigation.

The *lac* repressor is a paradigm of genetic control;[177] its ability to bind DNA and regulate gene expression is common to many regulatory proteins across all biological kingdoms.[11,12] The mechanisms by which LacI can arrest DNA into a looped configuration is a remarkable example of protein mechanics, in which a protein has to withstand large mechanical strain arising from forcing DNA into a looped configuration. Multiscale simulations have revealed which mechanical degrees of freedom are relevant to this task, allowing one to understand the underlying design of this class of proteins consisting of DNA binding domains linked by flexible linkers

to large protein cores.[204] The multiscale method can be used to study all possible DNA loop topologies induced by these regulatory proteins, besides that of LacI, also that of the *gal* repressor, another *E. coli* regulator that supposedly forms an antiparallel, *i.e.*, II/OO loop.[205] Future work will study the feasibility of these alternative topologies, characterize their properties, and asses the possibility of dynamical exchange between them.

References

1 J. Howard, *Mechanics of Motor Proteins and the Cytoskeleton*, Sinauer Associates, Inc., Sunderland, MA, 2001.
2 P. D. Boyer, *Annu. Rev. Biochem.*, 1997, **66**, 717–749.
3 M. Yoshida, E. Muneyuki and T. Hisabori, *Nat. Rev. Mol. Cell Biol.*, 2001, **2**, 669–677.
4 O. P. Hamill and B. Martinac, *Physiol. Rev.*, 2001, **81**(2), 685–740.
5 L. Tskhovrebova and J. Trinick, *Nat. Rev. Mol. Cell Biol.*, 2003, **4**(9), 679–689.
6 H. L. Granzier and S. Labeit, *Circ. Res.*, 2004, **94**, 284–295.
7 D. P. Corey and M. Sotomayor, *Nature*, 2004, **428**, 901–902.
8 D. P. Corey, J. García-Añoveros, J. R. Holt, K. Y. Kwan, S. Lin, M. A. Vollrath, A. Amalfitano, E. L.-M. Cheung, B. H. Derfler, D. A., G. S. G. Géléoc, P. A. Gray, M. P. Hoffman, H. L. Rehm, D. Tamasauskas and D. Zhang, *Nature*, 2004, **432**, 723–730.
9 R. O. Hynes, *Cell*, 2002, **110**, 673–687.
10 B. Geiger, A. Bershadsky, R. Pankov and K. Yamada, *Nat. Rev. Mol. Cell Biol.*, 2001, **2**, 793–805.
11 R. Schleif, *Annu. Rev. Biochem.*, 1992, **61**, 199–223.
12 K. S. Matthews, *Microbiol. Rev.*, 1992, **56**(1), 123–136.
13 E.-L. Florin, V. T. Moy and H. E. Gaub, *Science*, 1994, **264**, 415–417.
14 M. Rief, M. Gautel, F. Oesterhelt, J. M. Fernandez and H. E. Gaub, *Science*, 1997, **276**, 1109–1112.
15 K. Svoboda, C. Schmidt, B. Schnapp and S. Block, *Nature*, 1993, **365**, 721–727.
16 S. B. Smith, Y. Cui and C. Bustamante, *Science*, 1996, **271**, 795–799.
17 T. Ha, X. W. Zhuang, H. D. Kim, J. W. Orr, J. R. Williamson and S. Chu, *Proc. Natl. Acad. Sci. U. S. A.*, 1999, **96**(16), 9077–9082.
18 T. Ohashi, D. P. Kiehart and H. P. Erickson, *Proc. Natl. Acad. Sci. U. S. A.*, 1999, **96**, 2153–2158.
19 A. Yildiz, J. N. Forkey, S. A. McKinney, T. Ha, Y. E. Goldman and P. R. Selvin, *Science*, 2003, **300**(5628), 2061–2065.
20 R. Merkel, P. Nassoy, A. Leung, K. Ritchie and E. Evans, *Nature*, 1999, **397**, 50–53.

This journal is © the Owner Societies 2006

Phys. Chem. Chem. Phys., 2006, **8**, 3692–3706 | 3703

21 M. Carrion-Vazquez, A. Oberhauser, S. Fowler, P. Marszalek, S. Broedel, J. Clarke and J. Fernandez, *Proc. Natl. Acad. Sci. U. S. A.*, 1999, **96**, 3694–3699.

22 S. Izrailev, S. Stepaniants, M. Balsera, Y. Oono and K. Schulten, *Biophys. J.*, 1997, **72**, 1568–1581.

23 B. Isralewitz, S. Izrailev and K. Schulten, *Biophys. J.*, 1997, **73**, 2972–2979.

24 W. Wriggers and K. Schulten, *Proteins: Struct., Funct., Genet.*, 1999, **35**, 262–273.

25 D. Kosztin, S. Izrailev and K. Schulten, *Biophys. J.*, 1999, **76**, 188–197.

26 S. Izrailev, S. Stepaniants, B. Isralewitz, D. Kosztin, H. Lu, F. Molnar, W. Wriggers and K. Schulten, in *Computational Molecular Dynamics: Challenges, Methods, Ideas*, ed. P. Deuflhard, J. Hermans, B. Leimkuhler, A. E. Mark, S. Reich and R. D. Skeel, vol. 4 of Lecture Notes in Computational Science and Engineering, Springer-Verlag, Berlin, 1998, pp. 39–65.

27 M. V. Bayas, K. Schulten and D. Leckband, *Biophys. J.*, 2003, **84**, 2223–2233.

28 M. V. Bayas, K. Schulten and D. Leckband, *Mech. Chem. Biosystems*, 2004, **1**, 101–111.

29 D. Craig, M. Gao, K. Schulten and V. Vogel, *Structure*, 2004, **12**, 2049–2058.

30 H. Lu, B. Isralewitz, A. Krammer, V. Vogel and K. Schulten, *Biophys. J.*, 1998, **75**, 662–671.

31 H. Lu and K. Schulten, *Proteins: Struct., Funct., Genet.*, 1999, **35**, 453–463.

32 H. Lu and K. Schulten, *Chem. Phys.*, 1999, **247**, 141–153.

33 P. E. Marszalek, H. Lu, H. Li, M. Carrion-Vazquez, A. F. Oberhauser, K. Schulten and J. M. Fernandez, *Nature*, 1999, **402**, 100–103.

34 A. Krammer, H. Lu, B. Isralewitz, K. Schulten and V. Vogel, *Proc. Natl. Acad. Sci. U. S. A.*, 1999, **96**, 1351–1356.

35 H. Lu and K. Schulten, *Biophys. J.*, 2000, **79**, 51–65.

36 M. Gao, H. Lu and K. Schulten, *Biophys. J.*, 2001, **81**, 2268–2277.

37 D. Craig, A. Krammer, K. Schulten and V. Vogel, *Proc. Natl. Acad. Sci. U. S. A.*, 2001, **98**, 5590–5595.

38 M. Gao, M. Wilmanns and K. Schulten, *Biophys. J.*, 2002, **83**, 3435–3445.

39 A. Krammer, D. Craig, W. E. Thomas, K. Schulten and V. Vogel, *Matrix Biol.*, 2002, **21**, 139–147.

40 M. Gao, D. Craig, V. Vogel and K. Schulten, *J. Mol. Biol.*, 2002, **323**, 939–950.

41 M. Gao, D. Craig, O. Lequin, I. D. Campbell, V. Vogel and K. Schulten, *Proc. Natl. Acad. Sci. U. S. A.*, 2003, **100**, 14784–14789.

42 D. Craig, M. Gao, K. Schulten and V. Vogel, *Structure*, 2004, **12**, 21–30.

43 M. Sotomayor, D. P. Corey and K. Schulten, *Structure*, 2005, **13**, 669–682.

44 E. Villa, A. Balaeff and K. Schulten, *Proc. Natl. Acad. Sci. U. S. A.*, 2005, **102**, 6783–6788.

45 S. Izrailev, A. R. Crofts, E. A. Berry and K. Schulten, *Biophys. J.*, 1999, **77**, 1753–1768.

46 B. Isralewitz, J. Baudry, J. Gullingsrud, D. Kosztin and K. Schulten, *J. Mol. Graphics Modell.*, 2001, **19**, 13–25.

47 B. Isralewitz, M. Gao and K. Schulten, *Curr. Opin. Struct. Biol.*, 2001, **11**, 224–230.

48 H. Grubmüller, B. Heymann and P. Tavan, *Science*, 1996, **271**, 997–999.

49 A. Aksimentiev, I. A. Balabin, R. H. Fillingame and K. Schulten, *Biophys. J.*, 2004, **86**, 1332–1344.

50 I. Kosztin, R. Bruinsma, P. O'Lague and K. Schulten, *Proc. Natl. Acad. Sci. U. S. A.*, 2002, **99**, 3575–3580.

51 J. Gullingsrud, D. Kosztin and K. Schulten, *Biophys. J.*, 2001, **80**, 2074–2081.

52 M. Sotomayor and K. Schulten, *Biophys. J.*, 2004, **87**, 3050–3065.

53 E. Villa, A. Balaeff, L. Mahadevan and K. Schulten, *Multiscale Model. Simul.*, 2004, **2**, 527–553.

54 E. Paci and M. Karplus, *J. Mol. Biol.*, 1999, **288**, 441–459.

55 F. Gräter, J. Shen, H. Jiang, M. Gautel and H. Grubmüller, *Biophys. J.*, 2005, **88**, 790–804.

56 E. H. Lee, M. Gao, N. Pinotsis, M. Wilmanns and K. Schulten, *Structure*, 2006, **14**, 497–509.

57 P. Grayson, E. Tajkhorshid and K. Schulten, *Biophys. J.*, 2003, **85**, 36–48.

58 J. Stone, J. Gullingsrud, P. Grayson and K. Schulten, in *ACM Symposium on Interactive 3D Graphics*, ed. J. F. Hughes and C. H. Séquin, New York, 2001, pp. 191–194, ACM SIGGRAPH.

59 J. C. Phillips, R. Braun, W. Wang, J. Gumbart, E. Tajkhorshid, E. Villa, C. Chipot, R. D. Skeel, L. Kale and K. Schulten, *J. Comput. Chem.*, 2005, **26**, 1781–1802.

60 L. Li, H. H. Huang, C. L. Badilla and J. M. Fernandez, *J. Mol. Biol.*, 2005, **345**, 817–826.

61 J. Gullingsrud, R. Braun and K. Schulten, *J. Comput. Phys.*, 1999, **151**, 190–211.

62 K. Schulten, Z. Schulten and A. Szabo, *Physica A*, 1980, **100**, 599–614.

63 A. Szabo, K. Schulten and Z. Schulten, *J. Chem. Phys.*, 1980, **72**, 4350–4357.

64 K. Schulten, Z. Schulten and A. Szabo, *J. Chem. Phys.*, 1981, **74**, 4426–4432.

65 A. Oberhauser, C. Badilla-Fernandez, M. Carrion-Vazquez and J. Fernandez, *J. Mol. Biol.*, 2002, **319**, 433–447.

66 C. Jarzynski, *Phys. Rev. Lett.*, 1997, **78**, 2690–2693.

67 C. Jarzynski, *Phys. Rev. E: Stat. Phys., Plasmas, Fluids, Relat. Interdisc. Top.*, 1997, **56**, 5018–5035.

68 G. Hummer and A. Szabo, *Proc. Natl. Acad. Sci. U. S. A.*, 2001, **98**, 3658–3661.

69 S. Park and K. Schulten, *J. Chem. Phys.*, 2004, **120**, 5946–5961.

70 S. Park, K. Khalidi-Araghi, E. Tajkhorshid and K. Schulten, *J. Chem. Phys.*, 2003, **119**, 3559–3566.

71 M. Ø. Jensen, S. Park, E. Tajkhorshid and K. Schulten, *Proc. Natl. Acad. Sci. U. S. A.*, 2002, **99**, 6731–6736.

72 Y. Wang, K. Schulten and E. Tajkhorshid, *Structure*, 2005, **13**, 1107–1118.

73 S. Labeit and B. Kolmerer, *Science*, 1995, **270**, 293–296.

74 M. L. Bang, T. Centner, F. Fornoff, A. J. Geach, M. Gotthardt, M. McNabb, C. C. Witt, D. Labeit, C. C. Gregorio, H. Granzier and S. Labeit, *Circ. Res.*, 2001, **89**(11), 1065–1072.

75 K. Ma, L. S. Kan and K. Wang, *Biochemistry*, 2001, **40**(12), 3427–3438.

76 W. A. Linke, M. Ivemeyer, P. Mundel, M. R. Stockmeier and B. Kolmerer, *Proc. Natl. Acad. Sci. U. S. A.*, 1998, **95**(14), 8052–8057.

77 H. B. Li, A. F. Oberhauser, S. D. Redick, M. Carrion-Vazquez, H. P. Erickson and J. M. Fernandez, *Proc. Natl. Acad. Sci. U. S. A.*, 2001, **98**(19), 10682–10686.

78 A. Minajeva, M. Kulke, J. M. Fernandez and W. A. Linke, *Biophys. J.*, 2001, **80**, 1442–1451.

79 H. Li, W. Linke, A. F. Oberhauser, M. Carrion-Vazquez, J. G. Kerkvliet, H. Lu, P. E. Marszalek and J. M. Fernandez, *Nature*, 2002, **418**, 998–1002.

80 P. J. Zou, N. Pinotsis, M. Marino, S. Lange, A. Popov, I. Mavridis, M. Gautel, O. M. Mayans and M. Wilmanns, *Nature*, 2006, **439**, 229–233.

81 S. B. Fowler, R. B. Best, J. L. T. Herrera, T. J. Rutherford, A. Steward, E. Paci, M. Karplus and J. Clarke, *J. Mol. Biol.*, 2002, **322**(4), 841–849.

82 H. B. Li and J. M. Fernandez, *J. Mol. Biol.*, 2003, **334**(1), 75–86.

83 P. M. Williams, S. B. Fowler, R. B. Best, J. L. Toca-Herrera, K. A. Scott, A. Steward and J. Clarke, *Nature*, 2003, **422**(6930), 446–449.

84 M. Kellermayer, S. Smith, H. Granzier and C. Bustamante, *Science*, 1997, **276**, 1112–1116.

85 L. Tskhovrebova, J. Trinick, J. Sleep and R. Simmons, *Nature*, 1997, **387**, 308–312.

86 M. Gao, H. Lu and K. Schulten, *J. Muscle Res. Cell Motil.*, 2002, **23**, 513–521.

87 S. Improta, A. Politou and A. Pastore, *Structure*, 1996, **4**, 323–337.

88 H. Li, C. V. Mariano, A. F. Oberhauser, P. E. Marszalek and J. M. Fernandez, *Nat. Struct. Biol.*, 2001, **7**, 1117–1120.

89 E. Paci and M. Karplus, *Proc. Natl. Acad. Sci. U. S. A.*, 2000, **97**, 6521–6526.

90 D. K. Klimov and D. Thirumalai, *Proc. Natl. Acad. Sci. U. S. A.*, 1999, **96**, 1306–1315.

91 M. Cieplak, T. X. Hoang and M. O. Robbins, *Proteins: Struct., Funct., Genet.*, 2002, **49**(1), 114–124.

92 O. Mayans, J. Wuerges, S. Canela, M. Gautel and M. Wilmanns, *Structure*, 2001, **9**, 331–340.

93 M. Miller, H. Granzier, E. Ehler and C. Gregorio, *Trends Cell Biol.*, 2004, **14**, 119–126.
94 S. Lange, F. Xiang, A. Yakovenko, A. Vihola, P. Hackman, E. Rostkova, J. Kristensen, B. Brandmeier, G. Franzen, B. Hedberg, L. Gunnarsson, S. Hughes, S. Marchand, T. Sejersen, I. Richard, L. Edström, B. Udd and M. Gautel, *Science*, 2005, **308**, 1599–1603.
95 R. Knöll, M. Hoshijima, H. Hoffman, V. Person, I. Lorenzen-Schmidt, M. Bang, T. Hayashi, N. Shiga, H. Yasukawa, W. Schaper, W. McKenna, M. Yokoyama, N. Schork, H. Omens, A. McCulloch, A. Kimura, C. Gregorio, W. Poller, J. Schaper, H. Schultheiss and K. Chien, *Cell*, 2002, **111**, 943–955.
96 G. Valle, G. Faulkner, A. DeAntoni, P. Pacchioni, A. Pallavicini, D. Pandolfo, N. Tiso, S. Toppo, S. Trevisan and G. Lanfranchi, *FEBS Lett.*, 1997, **415**, 163–168.
97 C. C. Gregorio, K. Trombitas, T. Centner, B. Kolmerer, G. Stier, K. Kunke, K. Suzuki, F. Obermayr, B. Herrmann, H. Granzier, H. Sorimachi and S. Labeit, *J. Cell Biol.*, 1998, **143**(4), 1013–1027.
98 G. Faulkner, G. Lanfranchi and G. Valle, *Life*, 2001, **51**, 275–282.
99 R. Schroder, J. Reimann, A. Iakovenko, A. Mues, C. Bonne-mann, J. Matten and M. Gautel, *J. Muscle Res. Cell Motil.*, 2001, **22**, 259–264.
100 M. Itoh-Satoh, T. Hayashi, H. Nishi, Y. Koga, T. Arimura, T. Koyanagi, M. Takahashi, S. Hohda, K. Ueda, T. Nouchi, M. Hiroe, F. Marumo, T. Imaizumi, M. Yasunami and A. Kimura, *Biochem. Biophys. Res. Commun.*, 2002, **291**(2), 385–393.
101 M. Vainzof, E. Moreira, O. Suzuki, G. Faulkner, G. Valle, A. Beggs, O. Carpen, A. Ribeiro, E. Zanoteli, J. Gurgel-Giannetti, A. M. Tsanaclis, H. Silva, M. R. Passos-Bueno and M. Zatz, *Biochim. Biophys. Acta*, 2002, **1588**, 33–40.
102 C. Bonnemann and N. Laing, *Curr. Opin. Neurol.*, 2004, **17**, 529–537.
103 S. Laval and K. Bushby, *Neuropathol. Appl. Neurobiol.*, 2004, **30**, 91–105.
104 L. Tjernberg, D. Callaway, A. Tjernberg, S. Hahne, C. Lillie-hook, L. Terenius, J. Thyberg and C. Nordstedt, *J. Biol. Chem.*, 1999, **274**, 12619–12625.
105 D. Walsh, D. Hartley, M. Condron, M. Selkoe and D. Teplow, *Biochem. J.*, 2001, **355**, 869–877.
106 J. Karanicolas and C. Brooks, *Proc. Natl. Acad. Sci. U. S. A.*, 2003, **100**, 3555–3556.
107 J. Wang, S. Gülich, C. Bradford, M. Ramirez-Avarado and L. Regan, *Structure*, 2005, **13**, 1279–1288.
108 R. O. Hynes, *Fibronectins*, Springer-Verlag, New York, 1990.
109 Y. Mao and J. E. Schwarzbauer, *Matrix Biol.*, 2005, **24**(6), 389–399.
110 M. Shimaoka, J. Takagi and T. A. Springer, *Annu. Rev. Biophys. Biomol. Struct.*, 2002, **31**, 485–516.
111 D. J. Leahy, I. Aukhil and H. P. Erickson, *Cell*, 1996, **84**, 155–164.
112 A. Sharma, J. A. Askari, M. J. Humphries, E. Y. Jones and D. I. Stuart, *EMBO J.*, 1999, **18**, 1468–1479.
113 H. Erickson, *Proc. Natl. Acad. Sci. U. S. A.*, 1994, **91**, 10114–10118.
114 G. Baneyx, L. Baugh and V. Vogel, *Proc. Natl. Acad. Sci. U. S. A.*, 2002, **99**, 5139–43.
115 D. C. Hocking, J. Sottile and P. J. McKeown-Longo, *J. Biol. Chem.*, 1994, **269**, 19183–19187.
116 D. C. Hocking and K. Kowalski, *J. Cell Biol.*, 2002, **158**(1), 175–84.
117 J. L. Sechler, H. Rao, A. Cumiskey, I. Vega-Colon, M. Smith, T. Murata and J. Schwarzbauer, *J. Cell Biol.*, 2001, **154**, 1081–8.
118 K. C. Ingham, S. Brew, S. Huff and S. Litvinovich, *J. Cell Biochem.*, 1997, **272**, 1718–24.
119 S. V. Litvinovich, S. Brew, S. Aota, S. Akiyama, C. Haudenschild and K. Ingham, *J. Mol. Biol.*, 1998, **280**, 245–58.
120 D. C. Hocking, R. K. Smith and P. J. McKeown-Longo, *J. Cell Biol.*, 1996, **133**, 431–444.
121 H. Bultmann, A. Santas and D. Peters, *J. Biol. Chem.*, 1998, **273**, 2601–9.
122 A. Morla, Z. Zhang and E. Ruoslahti, *Nature*, 1994, **367**(6459), 193–6.
123 A. F. Oberhauser, P. E. Marszalek, H. Erickson and J. Fernandez, *Nature*, 1998, **393**, 181–185.
124 M. Rief, M. Gautel, A. Schemmel and H. Gaub, *Biophys. J.*, 1998, **75**, 3008–3014.
125 Y. Oberdorfer, H. Fuchs and A. Janshoff, *Langmuir*, 2000, **16**, 9955–9958.
126 S. P. Ng, R. W. S. Rounsevell, A. Steward, C. D. Geierhaas, P. M. Williams, E. Paci and J. Clarke, *J. Mol. Biol.*, 2005, **350**(4), 776–789.
127 K. Briknarova, M. E. Akerman, D. W. Hoyt, E. Ruoslahti and K. R. Ely, *J. Mol. Biol.*, 2003, **332**(1), 205–15.
128 E. Ruoslahti, *Annu. Rev. Cell Dev. Biol.*, 1996, **12**, 697–715.
129 R. P. Grant, C. Spitzfaden, H. Altroff, I. D. Campbell and H. J. Mardon, *J. Biol. Chem.*, 1997, **272**(10), 6159–6166.
130 F. Y. Li, S. D. Redick, H. P. Erickson and V. T. Moy, *Biophys. J.*, 2003, **84**(2), 1252–1262.
131 J. W. Lee, F. Ryan, J. C. Swaffield, S. A. Johnston and D. D. Moore, *Nature*, 1995, **374**, 91–94.
132 J. Emsley, C. G. Knight, R. W. Farndale, M. J. Barnes and R. C. Liddington, *Cell*, 2000, **101**(1), 47–56.
133 J. P. Xiong, T. Stehle, B. Diefenbach, R. Zhang, R. Dunker, D. L. Scott, A. Joachimiak, S. L. Goodman and M. A. Arnaout, *Science*, 2001, **294**, 339–345.
134 J. P. Xiong, T. Stehle, R. Zhang, A. Joachimiak, M. Frech, S. L. Goodman and M. A. Arnaout, *Science*, 2002, **296**, 151–155.
135 A. P. Mould, S. J. Barton, J. A. Askari, S. E. Craig and M. J. Humphries, *J. Biol. Chem.*, 2003, **278**(51), 51622–51629.
136 M. Gao and K. Schulten, *Biophys. J.*, 2006, **90**, 3267–3279.
137 P. G. Gillespie and R. G. Walker, *Nature*, 2001, **413**, 194–202.
138 A. J. Hudspeth and D. P. Corey, *Proc. Natl. Acad. Sci. U. S. A.*, 1977, **74**, 2407–2411.
139 D. P. Corey and A. J. Hudspeth, *J. Neurosci.*, 1983, **3**, 962–976.
140 E. Perozo, *Nat. Rev. Mol. Cell Biol.*, 2006, **7**, 109–119.
141 J. O. Pickles, S. D. Comis and M. P. Osborne, *Hear. Res.*, 1984, **15**, 103–112.
142 J. Howard and A. J. Hudspeth, *Neuron*, 1988, **1**, 189–199.
143 E. L. Cheung and D. P. Corey, *Biophys. J.*, 2005, **90**, 124–139.
144 P. G. Gillespie, R. A. Dumont and B. Kachar, *Curr. Opin. Neurol.*, 2005, **15**, 389–396.
145 J. Siemens, C. Lillo, R. A. Dumont, A. Reynolds, D. S. Williams, P. G. Gillespie and U. Müller, *Nature*, 2004, **428**, 950–955.
146 C. Söllner, G.-J. Rauch, J. Siemens, R. Geisler, S. C. Schuster, U. Müller and T. Nicolson, The Tübingen 2000 Screen Consortium, *Nature*, 2004, **428**, 955–958.
147 V. Tsuprun, R. J. Goodyear and G. P. Richardson, *Biophys. J.*, 2004, **87**, 4106–4112.
148 A. K. Rzadzinska, A. Derr, B. Kachar and K. Noben-Trauth, *Hear. Res.*, 2005, **208**, 114–121.
149 A. Lagziel, Z. M. Ahmed, J. M. Schultz, R. J. Morell, I. A. Belyantseva and T. B. Friedman, *Dev. Biol.*, 2005, **280**, 295–306.
150 V. Michel, R. J. Goodyear, D. Weil, W. Marcotti, I. Perfettini, U. Wolfrum, C. J. Kros, G. P. Richardson and C. Petit, *Dev. Biol.*, 2005, **280**, 281–294.
151 R. G. Walker, A. T. Willingham and C. S. Zuker, *Science*, 2000, **287**, 2229–2234.
152 S. Sidi, R. W. Friederich and T. Nicolson, *Science*, 2003, **301**, 96–99.
153 K. Nagata, A. Duggan, G. Kumar and J. Garcí a Añoveros, *J. Neurosci.*, 2005, **25**, 4052–4061.
154 L. Li, S. Wetzel, A. Pluckthun and J. M. Fernandez, *Biophys. J.*, 2006, **90**, L30–L32.
155 J. Shin, D. Adams, M. Paukert, M. Siba, S. Sidi, M. Levin, P. G. Gillespie and S. Gründer, *Proc. Natl. Acad. Sci. U. S. A.*, 2005, **102**, 12572–12577.
156 K. Y. Kwan, A. J. Allchorne, M. A. Vollrath, A. P. Christensen, D. S. Zhang, C. J. Woolf and D. P. Corey, *Neuron*, 2006, **50**, 277–289.
157 D. Bautista, S. E. Jordt, T. Nikai, P. R. Tsuruda, A. J. Read, E. N. Poblete, J. Yamoah, A. I. Basbaum and D. Julius, *Cell*, 2006, **124**, 1269–1282.
158 G. M. Story and R. W. Gereau, *Neuron*, 2006, **50**, 177–180.
159 J. Howard and S. Bechstedt, *Curr. Biol.*, 2004, **14**, 224–226.
160 W. Li, Z. Feng, P. W. Sternberg and X. Z. S. Xu, *Nature*, 2006, **440**, 684–687.
161 J. M. Bork, L. M. Peters, S. Riazuddin, S. L. Bernstein, Z. M. Ahmed, S. L. Ness, R. Polomeno, A. Ramesh, M. Schloss, C. R. S. Srisailpathy, D. Desmukh, Z. Ahmed, S. N. Khan, V. M. der

This journal is © the Owner Societies 2006

Phys. Chem. Chem. Phys., 2006, **8**, 3692–3706 | 3705

Kaloustian, X. C. Li, A. Lalwani, S. Riazuddin, M. Bitner-Glindzicz, W. E. Nance, X.-Z. Liu, G. Wistow, R. J. H. Smith, A. J. Griffith, E. R. Wilcox, T. B. Friedman and R. J. Morell, *Am. J. Hum. Genet.*, 2001, **68**, 26–37.

162 A. P. M. de Brouwer, R. J. Pennings, M. Roeters, P. van Hauwe, L. M. Astuto, L. H. Hoefsloot, P. L. M. Huygen, B. van den helm, A. F. Deutman, J. M. Bork, W. J. Kimberling, F. P. M. Cremers, C. W. R. J. Cremers and H. Kremer, *Hum. Genet.*, 2003, **112**, 156–163.

163 F. Di Palma, R. Pellegrino and K. Noben-Trauth, *Gene*, 2001, **281**, 31–41.

164 S. E. Lux, K. M. John and V. Bennett, *Nature*, 1990, **344**, 36–42.

165 S. E. Lux, W. T. Tse, J. C. Menninger, K. M. John, P. Harris, O. Shalev, R. R. Chilcote, S. L. Marchesi, P. C. Watkins, V. Bennett, S. Mcintosh, F. S. Collins, U. Francke, D. C. Ward and B. Forget, *Nature*, 1990, **345**, 736–739.

166 P. Bork, *Proteins: Struct., Funct., Genet.*, 1993, **17**, 363–374.

167 S. G. Sedgwick and S. J. Smerdon, *Trends Biochem. Sci.*, 1999, **24**, 311–316.

168 P. Michaely, D. R. Tomchick, M. Machius and R. G. W. Anderson, *EMBO J.*, 2002, **21**, 6387–6396.

169 M. R. Groves and D. Barford, *Curr. Opin. Struct. Biol.*, 1999, **9**, 383–389.

170 A. V. Kajava, *J. Biol. Chem.*, 2002, **277**, 49791–49798.

171 E. R. G. Main, S. E. Jackson and L. Regan, *Curr. Opin. Struct. Biol.*, 2003, **13**, 482–489.

172 T. J. Boggon, J. Murray, S. Chappuis-Flament, E. Wong, B. M. Gumbiner and L. Shapiro, *Science*, 2002, **296**, 1308–1313.

173 F. Cailliez and R. Lavery, *Biophys. J.*, 2005, **89**, 3895–3903.

174 G. Lee, K. Abdi, Y. Jiang, P. Michaely, V. Bennett and P. E. Marszalek, *Nature*, 2006.

175 T. J. Richmond and C. A. Davey, *Nature*, 2003, **423**, 145–150.

176 K. Heichman and R. Johnson, *Science*, 1990, **249**(4968), 511–517.

177 B. Müller-Hill, *The lac operon*, Walter de Gruyter, New York, 1996.

178 M. Lewis, G. Chang, N. C. Horton, M. A. Kercher, H. C. Pace, M. A. Schumacher, R. G. Brennan and P. Lu, *Science*, 1996, **271**, 1247–1254.

179 A. M. Friedman, T. O. Fischmann and T. A. Steitz, *Science*, 1995, **268**, 1721–1727.

180 B. Tolhuis, R. Palstra, E. Splinter, F. Grosveld and W. de Laat, *Mol. Cell*, 2002, **10**, 1453–1465.

181 M. Ptashne, *A Genetic Switch*, Cold Spring Harbor Laboratory Press, Cold Spring Harbor, NY, 2004.

182 *The Operon*, ed. J. H. Miller and W. S. Reznikoff, Cold Spring Harbor Laboratory Press, Cold Spring Harbor, NY, 1980.

183 J. Vilar and L. Saiz, *Curr. Opin. Genet. Dev.*, 2005, **15**, 136–144.

184 D. Swigon, B. D. Coleman and W. K. Olson, *Proc. Natl. Acad. Sci. U. S. A.*, 2006, **103**, 9879–9884.

185 A. Balaeff, L. Mahadevan and K. Schulten, *Phys. Rev. E: Stat. Phys., Plasmas, Fluids, Relat. Interdiscip. Top.*, 2006, **73**, 031919.

186 A. Balaeff, L. Mahadevan and K. Schulten, *Phys. Rev. Lett.*, 1999, **83**(23), 4900–4903.

187 A. Balaeff, C. R. Koudella, L. Mahadevan and K. Schulten, *Philos. Trans. R. Soc. London, Ser. A*, 2004, **362**, 1355–1371.

188 A. Balaeff, L. Mahadevan and K. Schulten, *Structure*, 2004, **12**, 123–132.

189 C. E. Bell and M. Lewis, *Nat. Struct. Biol.*, 2000, **7**(3), 209–214.

190 S. Oehler, E. R. Eismann, H. Krämer and B. Müller-Hill, *EMBO J.*, 1990, **9**(4), 973–979.

191 L. M. Edelman, R. Cheong and J. D. Kahn, *Biophys. J.*, 2003, **84**, 1131–1145.

192 L. Finzi and J. Gelles, *Science*, 1995, **267**, 378–380.

193 L. Bintu, N. Buchler, H. G. Garcia, U. Gerland, T. Hwa, J. Kondev, T. Kuhlman and R. Phillips, *Curr. Opin. Genet. Dev.*, 2005, **15**, 125–135.

194 J. W. Weisel, H. Shuman and R. I. Litvinov, *Curr. Opin. Struct. Biol.*, 2003, **13**(2), 227–235.

195 B. Marshall, M. Long, J. Piper, T. Yago, R. McEver and Z. C., *Nature*, 2003, **423**, 190–193.

196 J. M. Louis, I. J. Byeon, U. Baxa and A. M. Gronenborn, *J. Mol. Biol.*, 2005, **348**, 687–698.

197 M. Gao and K. Schulten, *Structure*, 2004, **12**, 2096–2098.

198 M. Jin, L. Andricioaei and T. A. Springer, *Structure*, 2004, **12**(12), 2137–2147.

199 E. Puklin-Faucher, M. Gao, K. Schulten and V. Vogel, *J. Cell Biol.*, 2006, submitted.

200 W. Schubert, C. Urbanke, T. Ziehm, V. Beier, M. P. Machner, E. Domann, J. Wehland, T. Chakraborty and d. W. Heinz, *Cell*, 2002, **111**, 825–836.

201 E. Conti, C. W. Muller and M. Stewart, *Curr. Opin. Struct. Biol.*, 2006, **16**(2), 237–244.

202 T. A. Isgro and K. Schulten, *Structure*, 2005, **13**, 1869–1879.

203 T. A. Isgro and K. Schulten, *J. Mol. Biol.*, 2006, submitted.

204 M. Weickert and S. Adhya, *J. Biol. Chem.*, 1992, **267**(22), 15869–15874.

205 M. Geanacopoulos, G. Vasmatzis, V. Zhurkin and S. Adhya, *Nat. Struct. Biol.*, 2001, **8**, 432–436.

206 W. Humphrey, A. Dalke and K. Schulten, *J. Mol. Graphics*, 1996, **14**, 33–38.